

Radiation-induced interaction of optical solitons in fibers with randomly varying birefringenceY. Chung,¹ V. V. Lebedev,² and S. S. Vergeles²¹*Theoretical Division, Los Alamos National Laboratory, Los Alamos, New Mexico 87545, USA*²*Landau Institute for Theoretical Physics, Kosygina 2, Moscow 119334, Russia*

(Received 5 January 2004; published 30 April 2004)

We study propagation of solitons in optical fibers with randomly varying birefringence which results in polarization mode dispersion. Due to the disorder, solitons emit radiation, i.e., the energy of the solitons is partly transferred into the delocalized modes. The radiation serves as a mediator of the intersoliton interaction leading to fluctuations of the soliton separations. We establish statistics of the fluctuations which is found to be sensitive to the phase mismatches and mutual polarizations of the solitons, and independent of the soliton separation. The theoretical results are justified by direct numerical simulations.

DOI: 10.1103/PhysRevE.69.046612

PACS number(s): 42.81.-i, 42.25.Dd

I. INTRODUCTION

Optical lines are widely used for transmission of information. Ideally, an information carried by optical pulses propagating through optical fibers would be transmitted undamaged. In reality, however, various impairments, emerging naturally in the transmission media, perturb the signal, which can lead to unrecoverable information losses. In modern high-speed fiber communications, the noise induced by optical amplifiers and the birefringent disorder caused by random variations in ellipticity of the fiber cross section are the two major origins of the transmission failure. While the amplifier noise is short correlated in time, the birefringence is practically frozen since the characteristic temporal scale of the birefringence disorder is long compared to the signal propagation time through the entire fiber line. A frequency dependence of the birefringence leads to splitting the optical pulse into two polarization components which propagate with slightly different velocities. This effect, in turn, results in pulse broadening known as polarization mode dispersion (PMD) [1–3]. Since the first report of this remarkable phenomenon, the PMD effect has been extensively studied experimentally [4–9] as well as theoretically [10–12].

In this paper, we investigate the role of the PMD impairment in the nonlinear regime of the information transmission when solitons are information carriers. Generally, the propagation of optical pulses is described by the coupled nonlinear Schrödinger equation derived in Ref. [13]. However, one should note that the birefringent disorder leads to fast random rotation of the principal axes of the polarization tensor along the fiber. Under certain conditions, this results in effective averaging of the Kerr nonlinearity [14–17]. Then the signal propagation can be described in terms of the Manakov equation [18]. The necessary conditions leading to this averaging process are established in Refs. [19–22]. Here, we assume that these conditions are well satisfied and therefore, base our consideration upon the Manakov equation supplemented by the term responsible for the PMD effect. The solitons (information carriers) correspond to the stationary solutions of the unperturbed Manakov equation. In the presence of the PMD disorder, however, the stationary nature of solitons is disturbed. In Ref. [23], the authors studied a direct influence of the disorder on the soliton propagation and re-

ported a phenomenon which can be called “direct soliton jitter.” While this effect is related to the direct impact of the disorder, there is another important feature in the soliton dynamics, which is produced indirectly by the fiber imperfections. Due to the disorder, solitons shed “radiation,” that is, the soliton energy is partly transferred into the delocalized modes. The emitted radiation spreads out from the soliton and influences other solitons, producing an effective intersoliton interaction. Under certain circumstances, this effect is more essential than the direct soliton jitter. Here, we focus mainly on this nondirect intersoliton interaction and analyze its statistical properties related to the PMD disorder.

In this study, we assume that the PMD disorder is weak, which is a necessary condition for successful information transmission. In the presence of weak disorder, the soliton parameters (position, width, polarization, phase, and phase velocity) undergo slow evolution along the fiber. On the other hand, the delocalized modes are relatively fast since there is a gap in the spectrum dividing the continuous spectrum from the modes corresponding to variations of the soliton parameters. This enables us to apply an adiabatic perturbation approach to find the evolution of the soliton parameters and radiation. In the case of single-soliton propagation, we examine the radiation profile and derive a soliton amplitude degradation law which is in accordance with one presented in Ref. [24]. Then, we make further progress and provide a role of the radiation shed by solitons. The major findings we report here concern fluctuations of soliton positions in the regime where the soliton energy loss is still negligible. The radiation emitted by solitons gives rise to intersoliton forces leading to random variations of the soliton separation. This effect is separation independent (we assume that the solitons are positioned far enough apart that no direct interaction occurs). We examine in detail this phenomenon in the context of the two-soliton evolution. Specifically, we provide the statistical characteristics of the intersoliton separation which can be treated as Gaussian jitter and its dependence on the phase mismatch and polarizations of the solitons. The extensive numerical simulations performed for two (parallel and orthogonal) polarizations and three different phase mismatches confirm our theoretical predictions. Then we discuss an extension of our results to the multisoliton propagation. The main feature in the multisoliton case is

an accumulation of the radiation effects discussed so far due to the separation independent intersoliton forces.

From the application point of view, this effect of radiation investigated here can be potentially dangerous especially in long-distance high-speed communication systems. In such systems, information is composed of sequences of pulses. As we mentioned earlier, the soliton displacement accumulates as the number of pulses increases. Consequently, this can produce an essential corruption of soliton patterns leading to communication errors.

The material in this paper is organized as follows. In Sec. II, the general theoretical setup is introduced. In Sec. III, we investigate the single-soliton evolution. In Sec. IV, the interaction of two solitons induced by radiation is analyzed. In Sec. V, the results of direct numerical simulations are presented and compared to the theoretical predictions. Finally, in Sec. VI, we summarize the main results of our analysis. Details of calculations are swept into appendixes.

II. GENERAL RELATIONS

The optical pulses propagating through a fiber can be described by the envelope $\Psi = (\Psi_1, \Psi_2)$ of electromagnetic field, which is a two-component complex quantity where components Ψ_1 and Ψ_2 stand for different polarization states of the optical signal. With the birefringent distortion and amplifier noise taken into account, the envelope Ψ satisfies the following equation [1,2,13,25]:

$$\begin{aligned} \partial_z \Psi - i\hat{\Delta}(z)\Psi - \hat{m}(z)\partial_t \Psi - id(z)\partial_t^2 \Psi - (4\gamma/3)i|\Psi|^2 \Psi \\ - (2\gamma/3)i\Psi^2 \Psi^* = \xi(z, t). \end{aligned} \quad (2.1)$$

Here and hereafter, asterisk denotes complex conjugation. In Eq. (2.1), z is the position along the fiber, t is the retarded time (measured in the reference frame moving with the optical signal), ξ represents the amplifier noise, d is the chromatic dispersion coefficient, and γ is the Kerr nonlinearity. The birefringent disorder is characterized by two random Hermitian 2×2 traceless matrices $\hat{\Delta}$ and \hat{m} (the latter one is related to the frequency dependence of the birefringence). The disorder is frozen at least on all the propagation related time scales, i.e., the matrices $\hat{\Delta}$ and \hat{m} can be treated as t independent.

Notice that there is no damping or amplification in Eq. (2.1). Such consideration is reasonable on scales larger than the interamplifier distance and under the condition that the amplification precisely compensates energy losses. Then we only have the noise ξ in Eq. (2.1), the amplifier leftover. Notice also that Eq. (2.1) is valid for a restricted number of optical channels since it is obtained by expanding the coefficients responsible for the chromatic dispersion and the birefringence near the carrier frequency.

The random matrix term, containing $\hat{\Delta}(z)$, can be excluded from the consideration by passing to the reference frame rotating together with local polarization states of the signal at the carrier frequency: $\Psi \rightarrow \hat{V}\Psi$, $\xi \rightarrow \hat{V}\xi$, and $\hat{m} \rightarrow \hat{V}\hat{m}\hat{V}^{-1}$. Here, the unitary matrix $\hat{V}(z)$ is the ordered exponential, $T \exp[i\int_0^z dz' \hat{\Delta}(z')]$, defined as the solution to the

equation, $\partial_z \hat{V} = i\hat{\Delta}\hat{V}$, with the initial condition $\hat{V}(0) = \hat{1}$. Hereafter, we use the notations \hat{m} , ξ , and Ψ for the transformed objects. We also neglect the variations of the chromatic dispersion d (the effects related to these variations were examined in Ref. [26]). Below, we use the dimensionless variables, assuming that the Kerr nonlinearity γ , the chromatic dispersion d , and soliton width are rescaled to unities.

Averaging over the polarization rotations, we obtain the following equation for the envelope of electromagnetic field describing signal propagation on scales larger than the birefringence correlation length (see Refs. [14–17] for more details),

$$i\partial_z \begin{pmatrix} \Psi_1 \\ \Psi_2 \end{pmatrix} + i\hat{m}\partial_t \begin{pmatrix} \Psi_1 \\ \Psi_2 \end{pmatrix} + \partial_t^2 \begin{pmatrix} \Psi_1 \\ \Psi_2 \end{pmatrix} + 2(|\Psi_1|^2 + |\Psi_2|^2) \begin{pmatrix} \Psi_1 \\ \Psi_2 \end{pmatrix} = 0. \quad (2.2)$$

Here, the contribution related to the additive noise is omitted (this contribution leads to the Elgin-Gordon-Haus effect [27,28] and can be examined separately). Equation (2.2) is the Manakov equation supplemented by an additional term (with the matrix \hat{m}) responsible for the PMD effect. The matrix \hat{m} is a random Hermitian 2×2 traceless matrix which can be written as

$$\hat{m} = h_1(z)\sigma_1 + h_2(z)\sigma_2 + h_3(z)\sigma_3, \quad (2.3)$$

where σ_i are Pauli matrices and $h_i(z)$ are real-valued functions of z .

We aim to examine the evolution of the soliton parameters averaged over the PMD disorder realizations. In the experimental setup, that corresponds to averaging over different fibers. Since the disorder gradually varies with time, such averaging process is equivalent to time averaging (for a given fiber) over intervals much larger than the characteristic time of the disorder variations.

Since the correlation length scale of the random fields $h_i(z)$ is short and all observable quantities can be expressed in terms of integrals along the line of $h_i(z)$, one can apply the central limit theorem (see, e.g., Ref. [29]) to the random fields. Hence, $h_i(z)$ can be treated as a Gaussian random variable, that is, its statistics can be characterized by the first correlation functions

$$\langle h_i \rangle = 0, \quad \langle h_j(z_1)h_k(z_2) \rangle = D\delta_{jk}\delta(z_1 - z_2), \quad (2.4)$$

where D represents the disorder intensity and $\langle \dots \rangle$ denotes the average over the disorder realizations. The zero mean of h_j and the isotropic character of its pair correlation function are related to the fast rotation produced by the matrix \hat{V} at the transformation $\hat{m} \rightarrow \hat{V}\hat{m}\hat{V}^{-1}$. Since we consider the case of weak PMD, i.e., $D \ll 1$, the integral $\mathbf{H} = \int dz \mathbf{h}(z)$ represents the PMD vector. As a consequence of Eq. (2.4), we find $\langle \mathbf{H}^2 \rangle = 3DZ$ where Z is the line length.

In the real optical lines, the line length is much larger than the soliton width, namely, $Z \gg 1$. Therefore, we focus on the domain $z \gg 1$ (where z is the coordinate along the fiber). Note that the product Dz can be small or large, depending on z . Here, we consider both cases.

The original Manakov equation, i.e., Eq. (2.2) with $\hat{m}=0$, is integrable and has exact solutions corresponding to N -soliton profiles for Ψ [18]. The PMD effect, however, disturbs the exact solutions. Nevertheless, if the disorder is weak, then the \hat{m} term in Eq. (2.2) can be treated as a small perturbation. Then there are solutions of this perturbed equation describing a set of localized pulses which we call, as for the “pure” Manakov equation, solitons.

Keeping in mind the nonlinear mode of the information transmission, we consider sequences of well separated single solitons, i.e., separations between the solitons are assumed to be essentially larger than their widths. Then the envelope Ψ can be written as

$$\Psi = \sum_n \Psi_n + \Psi_{con}, \quad (2.5)$$

where the terms Ψ_n describe the localized pulses (solitons) and the contribution Ψ_{con} represents the delocalized part of the optical signal (radiation).

We assume that at the input of the optical line (positioned at $z=0$), the signals are generated by the ideal solitons with the unitary widths (solutions of the pure Manakov equation). Then at $z=0$, we have

$$\Psi_n = \cosh^{-1}(t - y_n) \mathbf{e}_n, \quad (2.6)$$

and $\Psi_{con}=0$. Here, y_n are the “positions” (in time) of the solitons, and \mathbf{e}_n are the polarizations of the solitons satisfying the condition $\mathbf{e}_n^* \mathbf{e}_n = 1$. Say, for the linear polarization we have $\mathbf{e} = (e^{i\alpha}, 0)$, where α is the phase of the soliton and the first axis of the reference system is directed along the polarization vector. The expression (2.6) serves as the initial condition to Eq. (2.2).

Propagating along the line, the solitons evolve and radiation is emitted due to the PMD disorder. Because of the disorder weakness, the soliton evolution is slow, and hence, its shape adjusts adiabatically to an ideal profile. Therefore, the soliton evolution can be described in terms of the soliton parameters (amplitude, position, phase, phase velocity, and polarization) gradually varying along the line. On the contrary, the radiation evolves fast. Fortunately, due to the disorder weakness, the radiation can be examined in the framework of the perturbation theory.

We neglect the direct interaction between the solitons (since it is exponentially small if the solitons are well separated) whereas the interaction mediated by the radiation can be relevant. Hereafter, this nondirect interaction is the principal subject of our analysis.

III. SINGLE SOLITON

Since the solitons are assumed to be well separated, it is worth starting from the consideration of single soliton and radiation in its vicinity. For convenience, we redefine the phase and the polarization of radiation in accordance with the expression (2.5):

$$\begin{pmatrix} \Psi_1 \\ \Psi_2 \end{pmatrix} = \exp \left[i\alpha + i \int_0^z dz' \eta^2(z') + i\beta(t-y) \right] \\ \times \exp(-i\nu_0 \hat{\sigma}_2 + i\nu_2 \hat{\sigma}_1) \begin{bmatrix} 1 \\ 0 \end{bmatrix} \frac{\eta}{\cosh[\eta(t-y)]} \\ + \begin{pmatrix} v_1 \\ v_2 \end{pmatrix}. \quad (3.1)$$

The two-component field $\mathbf{v}=(v_1, v_2)$ in Eq. (3.1) describes the radiation emitted by the soliton due to the disorder. The quantities η , α , β , y represent the amplitude, phase, phase velocity, and position of the soliton, respectively, and $\nu_{0,2}$ describe the soliton polarizations.

In the absence of the disorder, η , α , β , and $\nu_{0,2}$ are z independent and y is a linear function of z : $y=y_0+2\beta z$ (where y_0 is the initial soliton position). Initially, $\eta=1$, $\beta=\nu_{0,2}=0$, in accordance with Eq. (2.6). The disorder causes variations of the soliton parameters along the line. Our aim is to find the equations governing this evolution.

A. Linear approximation

The radiation field \mathbf{v} has small amplitude because of the disorder weakness. Therefore, one can use the perturbation expansion over the disorder h_j and over the radiation field \mathbf{v} . This procedure can be constructed in spirit of the Kaup perturbation technique [30].

In this section, we examine the linear approximation. This implies that we consider the equations in the first order over the disorder h_j and the radiation \mathbf{v} . As we mentioned earlier, the changes of soliton parameters are slow. Hence, the quantities $\eta-1$, β , $\nu_{0,2}$, and $y-y_0$ which become nonzero due to the disorder should be treated as small parameters in this framework. We assume that the initial soliton polarization is linear and the first axis of the reference system is directed along the polarization vector.

By plugging the expression (3.1) into Eq. (2.2) and linearizing the resulting equation near the (unperturbed) localized part of the solution, we obtain the following set of equations for the radiation field \mathbf{v} :

$$i\partial_z \begin{pmatrix} v_1 \\ v_1^* \end{pmatrix} + \hat{L}_1 \begin{pmatrix} v_1 \\ v_1^* \end{pmatrix} + \dots = \begin{pmatrix} h_3 \\ h_3 \end{pmatrix} \frac{\tanh x}{\cosh x}, \quad (3.2)$$

$$i\partial_z \begin{pmatrix} v_2 \\ v_2^* \end{pmatrix} + \hat{L}_2 \begin{pmatrix} v_2 \\ v_2^* \end{pmatrix} + \dots = \begin{pmatrix} H \\ H^* \end{pmatrix} \frac{\tanh x}{\cosh x}, \quad (3.3)$$

$$\hat{L}_1 = (\partial_t^2 - 1)\hat{\sigma}_3 + \frac{2}{\cosh^2 x} (2\hat{\sigma}_3 + i\hat{\sigma}_2), \quad (3.4)$$

$$\hat{L}_2 = (\partial_t^2 - 1)\hat{\sigma}_3 + \frac{2}{\cosh^2 x} \hat{\sigma}_3, \quad (3.5)$$

where $x=t-y$ and the dots designate the terms originated from the derivatives of soliton parameters. Here we introduced a complex field

$$H(z) = h_1(z) + ih_2(z), \quad (3.6)$$

which possesses Gaussian statistics characterized by the pair correlation function

$$\langle H^*(z_1)H(z_2) \rangle = 2D\delta(z_1 - z_2). \quad (3.7)$$

Recall that D is the disorder intensity introduced by Eq. (2.4).

In order to solve Eqs. (3.2) and (3.3), it is convenient to expand the radiation field v over the eigenfunctions of the operators \hat{L}_1 and \hat{L}_2 [Eqs. (3.4) and (3.5)] which are presented in Appendix A. The eigenfunctions are separated into localized modes (corresponding to variations of the soliton parameters) and delocalized ones (corresponding to the radiation). The operator \hat{L}_1 has four localized modes, corresponding to the parameters y, β, α, η , and the operator \hat{L}_2 has two ones, corresponding to the polarization parameters v_0, v_2 . Projecting Eqs. (3.2) and (3.3) onto the delocalized eigenfunctions in accordance with the relations (A10) and (A17), one obtains the explicit equations for the expansion coefficients of the radiation field:

$$\begin{aligned} \frac{dy}{dz} - 2\beta &= h_3, & \frac{d\beta}{dz} &= 0, \\ \frac{d\alpha}{dz} &= 0, & \frac{d\eta}{dz} &= 0, \\ \frac{dv_0}{dz} &= \frac{dv_2}{dz} = 0. \end{aligned} \quad (3.8)$$

This is the system of equations valid in the linear approximation.

The solutions to Eqs. (3.8) with the initial condition (2.6) are $\alpha = \text{const.}, \beta = 0, \eta = 1, v_{0,2} = 0$, and $y = \int dz h_3$. Therefore, we obtain the average over the disorder realizations

$$\langle y^2 \rangle = Dz, \quad (3.9)$$

reproducing the soliton jitter reported in Ref. [23]. This effect can be called ‘‘direct jitter’’ since it is related to the direct influence of the disorder on the solitons.

B. Radiation

In this section, we investigate the profile of radiation shed by single soliton propagating along the line. In this case, the source of radiation is localized at the soliton and the radiation spreads in both directions from the soliton. We neglect the secondary source connected with the radiation itself, which is justified by the weakness of the disorder leading to small amplitude of the radiation. Thus, in the main approximation, the radiation can be examined in the first order over the disorder.

Here, we consider the regime where the soliton amplitude η can vary essentially during its propagation along the fiber. Then one needs to solve Eq. (2.2) linearized near the soliton with an arbitrary amplitude η . The eigenfunctions of the corresponding linear operators can be obtained by rescaling the

eigenfunctions of the operators (3.4) and (3.5) presented in Appendix A. Below we assume that $y=0$, i.e., placing the soliton position at the origin. The position fluctuations described by Eq. (3.9) are irrelevant for the problem. The reason is that in the linear approximation the position fluctuations are decoupled from the radiation, and, consequently, they influence the radiation in the second order over the disorder, which is outside our approximation.

We find that the modes corresponding to v_1 are not excited in the first order of h_j . Thus, in this approximation we only need to consider the field v_2 . This component of radiation field, v_2 , has the following expansion:

$$\begin{pmatrix} v_2 \\ v_2^* \end{pmatrix} = \int_{-\infty}^{+\infty} \frac{dk}{2\pi} [a_k \varphi_{k/\eta}(\eta t) + a_k^* \bar{\varphi}_{k/\eta}(\eta t)], \quad (3.10)$$

where $\varphi_k, \bar{\varphi}_k$ are the eigenfunctions defined by Eqs. (A15) and (A16) and a_k are complex-valued functions of z . Projecting the generalization of Eq. (3.3) onto the functions $\varphi_{k/\eta}, \bar{\varphi}_{k/\eta}$, one finds

$$\frac{da_k}{dz} - i(k^2 + \eta^2)a_k = \eta b_{k/\eta} H^*, \quad (3.11)$$

$$b_q = -\frac{\pi i(q+i)}{2 \cosh(\pi q/2)}. \quad (3.12)$$

Solving Eq. (3.11), we obtain

$$\begin{aligned} a_k(z) &= \int_0^z dz' b_{k/\eta(z')} \eta(z') H^*(z') \exp[ik^2(z-z')] \\ &+ i \int_{z'}^z dz'' \eta^2(z''). \end{aligned} \quad (3.13)$$

Considering the radiation far away from the soliton, i.e., in the region $t \gg \eta$, we find

$$\begin{aligned} v_2(z, t) &= \frac{1}{4} \int_0^z dz' \eta^2(z') \exp[-i \int_{z'}^z dz'' \eta^2(z'')] \\ &\times \mathcal{J}[\eta(z')t, \eta^2(z')(z-z')] H(z'), \end{aligned} \quad (3.14)$$

where

$$\mathcal{J}(x, s) = \int_{-\infty}^{+\infty} dq \frac{1+iq}{\cosh(\pi q/2)} e^{(-iqx - iq^2s)}. \quad (3.15)$$

A stationary phase calculation of the above integral yields

$$\mathcal{J}(x, s) \approx \sqrt{\frac{\pi}{is}} \left(1 - i \frac{x}{2s}\right) \frac{\exp(ix^2/4s)}{\cosh(\pi x/4s)}, \quad (3.16)$$

which is valid at $s \gg 1$.

Equation (3.14) shows that v_2 , as a linear combination of H , possesses Gaussian statistics with zero average. Therefore, the stochastic properties of the radiation field can be characterized by its mean square fluctuations. Multiplying two replicas of Eq. (3.14) and averaging the result over the disorder in accordance with Eqs. (3.6) and (3.7), we find

$$\langle |v_2|^2 \rangle = \frac{D}{8} \int_0^z dz' \eta^4(z') |\mathcal{J}[\eta(z')t, \eta^2(z')(z-z')]|^2. \quad (3.17)$$

To examine the average (3.17) in more detail, we have to establish a z dependence of the soliton amplitude η , which is the subject of the following section.

Note that above we neglected the terms originated from $\partial_z \eta$. In other words, we used the adiabatic approximation for the radiation. It is justified by the fact that $\partial_z \eta$ appears in the second order of the disorder whereas we examine the radiation field in the first order of the disorder.

C. Soliton degradation law

In this section, we derive a degradation law for the single-soliton propagation. Previously, we found that the amplitude of the soliton remains unchanged in the linear approximation of the disorder. Therefore, to find the law, one has to take into account the second order of the disorder. Since we consider essential variations of the amplitude, we need to use for the radiation the adiabatic approach developed in the preceding section.

To establish the soliton degradation law, it is convenient to start from the conservation law

$$\partial_z |\Psi|^2 = i \partial_t (\Psi^* \partial_t \Psi - \Psi \partial_t \Psi^*) - \partial_t (\Psi^* \hat{m} \Psi), \quad (3.18)$$

following from Eq. (2.2). Now the localized nature of the soliton can be used. We first integrate both sides of Eq. (3.18) over $-\tau \leq t \leq \tau$, where $\tau \gg \eta$. Then one finds that the major contribution to the integral $\int_{-\tau}^{\tau} dt |\Psi(t)|^2$ comes from the soliton and hence, becomes 2η . The integral of the right-hand side of Eq. (3.18) involves the boundary value evaluations. On the boundaries, $t = -\tau, \tau$, we can keep only the radiation term in the expression (3.1). Then we obtain

$$\frac{d\eta}{dz} = i(\mathbf{v}^* \partial_t \mathbf{v} - \mathbf{v} \partial_t \mathbf{v}^*)|_{t=\tau}. \quad (3.19)$$

Here, we omitted the contribution related to the last term in Eq. (3.18) and the t dependence of the factors in Eq. (3.1) since they are of the third order over the disorder h_j .

As it follows from Eq. (3.14), the right-hand side of Eq. (3.19) is determined by the integrals of the random disorder h_j and, consequently, it is a self-averaging quantity. Therefore, in the main approximation, the right-hand side of Eq. (3.19) can be substituted by its average value. Plugging Eq. (3.14) into Eq. (3.19) and averaging over the disorder, we find

$$\frac{d\eta}{dz} = \frac{Di}{4} \int_0^z dz' \eta^4(z') \mathcal{J}^* \partial_\tau \mathcal{J},$$

where $\mathcal{J} = \mathcal{J}[\eta(z')\tau, \eta^2(z')(z-z')]$. The function \mathcal{J} can be approximated by its asymptotic value (3.16), which yields

$$\frac{d\eta}{dz} = -\frac{\pi D}{4} \int_0^z dz' \frac{\tau \eta^2(z')}{(z-z')^2 \cosh^2(\pi \zeta/2)},$$

where $\zeta = \tau/[\eta(z')(z-z')]$. Then, calculating the integral over $[0, z]$ (it can be extended from $-\infty$ to $+\infty$ because of the inequality $\tau \gg \eta$) we obtain the equation $d\eta/dz = -2D\eta^3/3$ leading to the solution

$$\eta(z) = \left(1 + \frac{4D}{3}z\right)^{-1/2}. \quad (3.20)$$

Thus, the soliton asymptotically decays as $\eta \propto z^{-1/2}$ due to the PMD disorder, which is in agreement with Ref. [24]. It is instructive to compare the law (3.20) with one caused by the chromatic disorder which gives the asymptotic behavior $\eta \propto z^{-1/4}$ [26].

Now we return to Eq. (3.17). Using the expression for the soliton amplitude (3.20), we can obtain the space and time dependence of the mean square fluctuation of the radiation. From the formulas (3.15) and (3.16), one finds the following expressions in different spatial-temporal domains

$$Dz \ll 1, z \gg t \gg 1: \quad \langle |v_2|^2 \rangle = \frac{\pi D}{8} \ln(z/t),$$

$$Dz \ll 1, t \gg z \gg 1: \quad \langle |v_2|^2 \rangle = \frac{Dt}{16z} \exp\left(-\frac{\pi t}{2z}\right),$$

$$Dz \gg 1, t^2 \ll z/D: \quad \langle |v_2|^2 \rangle = \frac{3\pi}{64z} \ln \frac{Dz^3}{t^2},$$

$$Dz \gg 1, z \gg t \gg \sqrt{z/D}: \quad \langle |v_2|^2 \rangle = \frac{3\pi}{16z} \ln(z/t),$$

$$Dz \gg 1, t \gg z: \quad \langle |v_2|^2 \rangle = \frac{3t}{32z^2} \exp\left(-\frac{\pi t}{2z}\right).$$

The above expressions show that the mean square fluctuation of the radiation has the logarithmic profile at $t < z$ and decays exponentially at $t > z$.

Let us reproduce here a short qualitative explanation of this behavior given in Ref. [26]. The radiation emitted by the soliton can be represented as a series of Fourier harmonics with the frequencies k : $\mathbf{v}_k \propto \exp(-i\lambda_k z + ikt)$. The dispersion law, valid for the propagation of the radiation in the linear regime, is $\lambda_k = 1 + k^2$, leading to the group velocity $dt/dz = 2k$. Since the radiation source localized at the soliton initially has the amplitude 1, Fourier harmonics have approximately equal amplitudes at $k \lesssim 1$, and their amplitudes diminish fast as k increases in the domain $k \gtrsim 1$. Therefore there is a small number of wave packets running more than $t \sim z$ (this explains the exponential decay at $t > z$). The logarithmic dependence of the profile in the region $t < z$ reflects the number of wave packets reaching a given t at some z .

We obtained the degradation law (3.20) for a single-soliton propagation. It is clear that the same degradation law can be observed for a multisoliton pattern provided the solitons are well separated. The reason is that the degradation

law reflects the energy losses of soliton due to the imperfections of the fiber. This is evidently a “single-particle” process. Notice that the soliton amplitude remains practically unchanged in the region $Dz \ll 1$. Hereafter, our analysis is focused on this domain, keeping a direct relation to the information transmission in real optical lines.

D. Forces and impulses

This section is devoted to the role of radiation in soliton propagation. Assuming that $Dz \ll 1$, we examine the evolution of soliton parameters under the action of the radiation. For this purpose, we need an accuracy up to $O(h_j^2)$. Again, we suppose that initially the soliton has linear polarization and that the first axis of the reference system is directed along the polarization.

Equation (3.8) shows that the equation for the soliton position y is coupled to the equation for the phase velocity β already in the first order over h_j , \mathbf{v} . Thus, we need to find the second-order corrections over h_j , \mathbf{v} to the equations for y and β . It also follows from Eq. (3.8) that corrections to η , α , and $\nu_{0,2}$ can appear only in the second order over h_j . Such corrections produce contributions $O(h_j^3)$ to the equations for y and β , which are negligible in our approximation. Therefore, we can ignore these corrections, substituting $\eta=1$, $\nu_{0,2}=0$, and letting α be some constant in the expression (3.1).

Expanding Eq. (2.2) up to the second order over h_j , \mathbf{v} and projecting the result onto the corresponding eigenfunctions of the operator (3.4) (see Appendix A), we obtain

$$\frac{d\beta}{dz} = \mathcal{F} = \Phi_{vv} + \mathcal{F}_{vv} + \mathcal{F}_{vh}, \quad (3.21)$$

$$\frac{dy}{dz} = h_3 + \mathcal{P}, \quad \mathcal{P} = 2\beta + \mathcal{P}_{vv} + \mathcal{P}_{vh}, \quad (3.22)$$

where both the first- and the second-order terms are kept. One can say that \mathcal{F} is the force acting on the soliton and that $h_3 + \mathcal{P}_{vv} + \mathcal{P}_{vh}$ is an extra impulse. The explicit expressions for the contributions to the force and to the impulse are

$$\mathcal{F}_{vv} = 2 \int dt \frac{\tanh x}{\cosh^2 x} |v_2|^2, \quad (3.23)$$

$$\mathcal{F}_{vh} = -\text{Im} \left(H^* \int dt \frac{\tanh x}{\cosh x} \partial_t v_2 \right), \quad (3.24)$$

$$\Phi_{vv} = \int dt \frac{\tanh x}{\cosh^2 x} [4|v_1|^2 + v_1^2 + (v_1^*)^2], \quad (3.25)$$

$$\mathcal{P}_{vv} = i \int dt \frac{x}{\cosh^2 x} [v_1^2 - (v_1^*)^2], \quad (3.26)$$

$$\mathcal{P}_{vh} = -\text{Re} \left(H^* \int dt \frac{x}{\cosh x} \partial_t v_2 \right), \quad (3.27)$$

where $x=t-y$. Since the integrals are determined by a narrow vicinity of the soliton, the integration over t can be extended from $-\infty$ to $+\infty$.

If we substitute the formula (3.14) (with $\eta=1$) into the above expressions, then we obtain zero values of the contributions to the force and impulse (excluding the first-order term h_3). This is a manifestation of the absence of the soliton self-action. For a multisoliton pattern, however, the contributions to the force and to the impulse are nonzero, depending on the characteristics of the soliton pattern. Thus, the radiation becomes a mediator of the intersoliton interaction. In the following section, we examine in detail the interaction of solitons and radiation at the onset of two-soliton pattern.

IV. TWO SOLITONS

In this section, we consider two-soliton dynamics. From Eq. (3.20), one finds that solitons start to degrade in the region $z \sim 1/D$. Here, we focus on the domain $z \ll 1/D$ where the degradation effect is negligible and hence, the amplitudes of the solitons can be treated as unchanged. We are mainly interested in the fluctuations of the separation between the solitons which can be a potential source of the information losses.

We consider the solitons 1 and 2 positioned at y_1 and y_2 ($y_2 > y_1$) with the separation $y=y_2-y_1$ which is assumed to be much larger than unity. Then, one can neglect the direct interaction between the solitons (which is exponentially small) and take into account only the interaction mediated by the radiation. In the two-soliton dynamics, the contribution Ψ_{con} in Eq. (2.5), related to the radiation, is a superposition of two terms, corresponding to the radiation emitted by each soliton. In this case the impulses and the forces applied to the solitons are nonzero. Below, we examine the soliton position shifts induced by the radiation and their dependence on the phase mismatch and polarization of the solitons (which are assumed to be linearly polarized). The phase mismatch $\alpha = \alpha_2 - \alpha_1$ (where α_1 and α_2 are phases of the solitons) is arbitrary and we consider two cases: parallel and orthogonal polarizations.

A. Solitons with parallel polarizations

We first consider the case when both solitons are initially polarized identically. Then, the expression (2.5) can be rewritten as

$$\begin{pmatrix} \Psi_1 \\ \Psi_2 \end{pmatrix} = \exp(iz + i\alpha_1) \left\{ \left[\frac{\exp(i\beta_1 x_1)}{\cosh(x_1)} + \frac{\exp(i\beta_2 x_2 + i\alpha)}{\cosh(x_2)} \right] \begin{pmatrix} 1 \\ 0 \end{pmatrix} + \begin{pmatrix} v_1 \\ v_2 \end{pmatrix} \right\}, \quad (4.1)$$

in spirit of Eq. (3.1). Here and hereafter, $x_1=t-y_1$ and $x_2=t-y_2$. In accordance with aforesaid, we set the amplitudes $\eta_1 = \eta_2 = 1$ and neglected the degrees of freedom responsible for the fluctuations of polarizations. The phase mismatch α

can be treated as a parameter which does not undergo changes along the fiber.

In order to obtain the forces and impulses in accordance with Eqs. (3.21)–(3.27), one needs to find the radiation field \mathbf{v} , which can be examined in the linear approximation. Substituting the expression (4.1) into Eq. (2.2) and linearizing the equation in \mathbf{v} and h_j (and neglecting β_1, β_2), we find

$$\partial_z \begin{pmatrix} v_2 \\ v_2^* \end{pmatrix} - i\hat{\mathcal{L}}_2 \begin{pmatrix} v_2 \\ v_2^* \end{pmatrix} = \begin{pmatrix} H \\ H^* \end{pmatrix} \frac{\tanh(x_1)}{\cosh(x_1)} + \begin{pmatrix} He^{i\alpha} \\ H^* e^{-i\alpha} \end{pmatrix} \frac{\tanh(x_2)}{\cosh(x_2)}, \quad (4.2)$$

where the operator $\hat{\mathcal{L}}_2$ is a generalization of the operator \hat{L}_2 , defined by Eq. (3.5). Near the first soliton, $\hat{\mathcal{L}}_2$ coincides with \hat{L}_2 , and near the second soliton, $\hat{\mathcal{L}}_2$ differs from \hat{L}_2 by some phase factors. Similar to the single-soliton case, the component v_1 is not excited in this approximation and hence, we can neglect this component of the radiation field.

Again, we solve Eq. (4.2) by expanding the field v_2 over the eigenfunctions of the operator $\hat{\mathcal{L}}_2$, corresponding to the delocalized solutions. The eigenfunctions φ_{\parallel} of $\hat{\mathcal{L}}_2$ can be written as

$$\begin{aligned} t < (y_1 + y_2)/2, \quad \varphi_{k\parallel} &= \varphi_k(x_1), \quad \bar{\varphi}_{k\parallel} = \bar{\varphi}_k(x_1), \\ t > (y_1 + y_2)/2, \quad \varphi_{k\parallel} &= \frac{k+i}{k-i} e^{iky} \varphi_k(x_2), \\ \bar{\varphi}_{k\parallel} &= \frac{k-i}{k+i} e^{-iky} \bar{\varphi}_k(x_2), \end{aligned} \quad (4.3)$$

where the functions φ_k and $\bar{\varphi}_k$ are introduced in Sec. II of Appendix A. In the region between the solitons, the expressions (4.3) match well. Expanding v_2 by the continuous spectrum only, we find

$$\begin{pmatrix} v_2 \\ v_2^* \end{pmatrix} = \int_{-\infty}^{+\infty} \frac{dk}{2\pi} (a_{k\parallel} \varphi_{k\parallel} + a_{k\parallel}^* \bar{\varphi}_{k\parallel}), \quad (4.4)$$

where $a_{k\parallel}$ are complex-valued functions of z .

Then, projecting Eq. (4.2) to the eigenfunctions (4.3), we obtain

$$\frac{d}{dz} a_{k\parallel} - i(k^2 + 1)a_{k\parallel} = b_k H^*(z) \left[1 + \frac{k-i}{k+i} e^{-iky-i\alpha} \right],$$

where b_k are defined in Eq. (3.12). The solution of the above equation is

$$\begin{aligned} a_{k\parallel}(z) &= b_k \int_0^z dz' \exp[i(k^2 + 1)(z - z')] \\ &\times \left[1 + \frac{k-i}{k+i} e^{-iky-i\alpha} \right] H^*(z'), \end{aligned} \quad (4.5)$$

similar to Eq. (3.13).

Substituting the formulas (4.3)–(4.5) into Eqs. (3.23)–(3.27), we obtain explicit expressions for the forces and impulses in terms of h_j . Then we can analyze statistical

properties of the forces and impulses starting from Eq. (2.4) (the details of the analysis are presented in Appendix B). The average value of \mathcal{F} is exponentially small (proportional to the factor e^{-y} , where y is the intersoliton separation) and can be neglected. The average value of \mathcal{P} is $D/4$ [see Eq. (B11)] which gives a systematic drift $\Delta y_{1,2} = (D/4)z$ of the soliton positions. As we will show below, it is a subleading contribution to the variation of the separation, δy . Thus, we focus on the pair correlation functions of the quantities.

For the impulse of the first soliton, we find

$$\langle \mathcal{P}_1(z_1) \mathcal{P}_1(z_2) \rangle = 4G_{\parallel} D^2 \min(z_1, z_2), \quad (4.6)$$

where the average value of \mathcal{P}_1 is neglected. G_{\parallel} in Eq. (4.6) is a numerical constant: $G_{\parallel} \approx 0.204$. Now let us turn to the fluctuation of the impulse differences between the solitons. We find [see Eq. (B15)]

$$\begin{aligned} \langle [\mathcal{P}_2(z_1) - \mathcal{P}_1(z_1)] [\mathcal{P}_2(z_2) - \mathcal{P}_1(z_2)] \rangle \\ = 8[1 + \cos(2\alpha)] G_{\parallel} D^2 \min(z_1, z_2), \end{aligned} \quad (4.7)$$

where the subscripts 1 and 2 correspond to the first and the second solitons.

Now we establish the statistics of the fluctuations $\delta y_1, \delta y_2$, and δy of the soliton positions y_1, y_2 and the separation $y = y_2 - y_1$, respectively. As it follows from Eq. (4.7), the second-order moments are

$$\langle (\delta y_{1,2})^2 \rangle = \frac{4}{3} G_{\parallel} D^2 z^3 + Dz, \quad (4.8)$$

$$\langle (\delta y)^2 \rangle = \frac{8}{3} [1 + \cos(2\alpha)] G_{\parallel} D^2 z^3. \quad (4.9)$$

Note that the term Dz in $\langle (\delta y_{1,2})^2 \rangle$ is induced by the first-order contribution to the impulse, h_3 , in the right-hand side of Eq. (3.22). This term corresponds to the expression (3.9). Equations (4.8) and (4.9) show that the relative position shift is sensitive to the phase mismatch α . The systematic drift $\Delta y_{1,2} = (D/4)z$ of the soliton positions is negligible in comparison to the typical fluctuation of the separation $\delta y \sim Dz^{3/2}$ at $z \gg 1$, which justifies neglecting the drift. Hence, the typical displacement caused by the pair soliton interaction is proportional to $z^{3/2}$ which is similar to the Elgin-Gordon-Haus jitter [27,28].

We remark that the high-order irreducible correlation functions of the force \mathcal{F} and the impulse \mathcal{P} only produce small corrections to the moments of $\delta y_{1,2}$ and δy provided $z \gg 1, Dz \ll 1$. Therefore, the fluctuations of soliton positions possess Gaussian statistics, which can be completely characterized by Eqs. (4.8) and (4.9).

B. Solitons with orthogonal polarizations

We now turn to the case when solitons have orthogonal polarizations. In this case, the expression (4.1) has to be replaced by

$$\begin{pmatrix} \Psi_1 \\ \Psi_2 \end{pmatrix} = \exp(iz + i\alpha_1) \left\{ \frac{\exp(i\beta_1 x_1)}{\cosh(x_1)} \begin{pmatrix} 1 \\ 0 \end{pmatrix} + \frac{\exp(i\beta_2 x_2 + i\alpha)}{\cosh(x_2)} \begin{pmatrix} 0 \\ 1 \end{pmatrix} + \begin{pmatrix} v_1 \\ v_2 \end{pmatrix} \right\}, \quad (4.10)$$

again in spirit of Eq. (3.1). Following a procedure similar to one developed in the preceding section, we find

$$i\partial_z \begin{pmatrix} v_1 \\ v_1^* \end{pmatrix} + \hat{\mathcal{L}}_I \begin{pmatrix} v_1 \\ v_1^* \end{pmatrix} = ih_3 f_1(x_1) + i\hat{H}^* \hat{\Theta}^{-1} f_1(x_2), \quad (4.11)$$

$$i\partial_z \begin{pmatrix} v_2 \\ v_2^* \end{pmatrix} + \hat{\mathcal{L}}_{II} \begin{pmatrix} v_2 \\ v_2^* \end{pmatrix} = i\hat{H} f_1(x_1) - ih_3 \hat{\Theta}^{-1} f_1(x_2), \quad (4.12)$$

where

$$\hat{H} = \begin{pmatrix} H & 0 \\ 0 & H^* \end{pmatrix}, \quad \hat{\Theta} = \begin{pmatrix} e^{i\alpha} & 0 \\ 0 & e^{-i\alpha} \end{pmatrix}.$$

Here, f_1 is defined in Appendix A and the operators $\hat{\mathcal{L}}_I$ and $\hat{\mathcal{L}}_{II}$ are linearized parts of Eqs. (2.2), analogous to the operators $\hat{\mathcal{L}}_{1,2}$ [Eqs. (3.4) and (3.5)]. Note that in the case of orthogonal polarization, both components of the radiation field, v_1 and v_2 , are relevant.

Equations (4.11) and (4.12) can be solved after expanding the fields v_1 and v_2 over the eigenfunctions of the operators $\hat{\mathcal{L}}_I$ and $\hat{\mathcal{L}}_{II}$, respectively:

$$\begin{pmatrix} v_1 \\ v_1^* \end{pmatrix} = \int_{-\infty}^{+\infty} \frac{dk}{2\pi} (a_{k\perp} f_{k\perp} + a_{k\perp}^* \bar{f}_{k\perp}), \quad (4.13)$$

$$\begin{pmatrix} v_2 \\ v_2^* \end{pmatrix} = \int_{-\infty}^{+\infty} \frac{dk}{2\pi} (c_{k\perp} \varphi_{k\perp} + c_{k\perp}^* \bar{\varphi}_{k\perp}), \quad (4.14)$$

where $a_{k\perp}, c_{k\perp}$ are complex-valued functions of z . Here, the eigenfunctions are

$$\begin{aligned} t < (y_1 + y_2)/2, & \quad f_{k\perp} = f_k(x_1), \quad \bar{f}_{k\perp} = \bar{f}_k(x_1), \\ t > (y_1 + y_2)/2, & \quad f_{k\perp} = \frac{k+i}{k-i} e^{iky} \varphi_k(x_2), \end{aligned} \quad (4.15)$$

$$\bar{f}_{k\perp} = \frac{k-i}{k+i} e^{-iky} \bar{\varphi}_k(x_2),$$

$$t < (y_1 + y_2)/2, \quad \varphi_{k\perp} = \varphi_k(x_1), \quad \bar{\varphi}_{k\perp} = \bar{\varphi}_k(x_1),$$

$$t > (y_1 + y_2)/2, \quad \varphi_{k\perp} = \frac{(k+i)^2}{(k-i)^2} e^{iky+i\alpha} \hat{\Theta} f_k(x_2),$$

$$\bar{\varphi}_{k\perp} = \frac{(k-i)^2}{(k+i)^2} e^{-iky-i\alpha} \hat{\Theta} \bar{f}_k(x_2), \quad (4.16)$$

where $f_k, \varphi_k, \bar{f}_k, \bar{\varphi}_k$ are defined in Appendix A. Again, the expressions smoothly match in the region between the solitons. Using the expressions (4.13) and (4.14), we find

$$\begin{aligned} \frac{d}{dz} a_{k\perp} - i(k^2 + 1)a_{k\perp} &= b_k H(z) \frac{k-i}{k+i} e^{-iky-i\alpha}, \\ \frac{d}{dz} c_{k\perp} - i(k^2 + 1)c_{k\perp} &= b_k H^*(z), \end{aligned} \quad (4.17)$$

and b_k is defined in Eq. (3.12). The solutions of Eqs. (4.17) are

$$a_{k\perp} = b_k \int_0^z dz' H(z') \frac{k-i}{k+i} e^{-iky-i\alpha} e^{i(k^2+1)(z-z')}, \quad (4.18)$$

$$c_{k\perp} = b_k \int_0^z dz' H^*(z') e^{i(k^2+1)(z-z')}. \quad (4.19)$$

In the case of orthogonal polarizations, some terms in Eqs. (3.21) and (3.22) are found to be zero, see Appendix C. An analysis made in this appendix shows that the main effect related to the second-order terms is produced by the average $\langle \mathcal{P}_1 \rangle \sim D$, leading to the systematic drift $\Delta y_{1,2} \approx 0.6Dz$. This drift is negligible compared to the fluctuations of the positions. Therefore the term with β_1 can be neglected in Eq. (3.22) for y_1 . The term \mathcal{P}_{vw} can be also neglected in comparison with h_3 (see Appendix C). As a result, we return to the first-order equation $\partial_z y_1 = h_3$, and similarly, $\partial_z y_2 = -h_3$. Hence, we obtain

$$\langle (\delta y_{1,2})^2 \rangle = Dz, \quad (4.20)$$

$$\langle (\delta y)^2 \rangle = 4Dz. \quad (4.21)$$

Notice that the result (4.20) coincides with Eq. (3.9). In contrast to the parallel polarization case, there is no α dependence in the second-order moments. We also note that the terms proportional to z^3 are absent. For more details of the calculation concerning the forces and impulses, we refer the reader to Appendix C.

Again, one can check that the high-order irreducible correlation functions of the impulse \mathcal{P} [see Eq. (C12)] produce small corrections to the moments of $\delta y_{1,2}$ and δy provided $z \gg 1, Dz \ll 1$. Thus, the fluctuations of soliton positions possess Gaussian statistics and can be completely characterized by Eqs. (4.20) and (4.21).

C. Arbitrary polarizations

The forces and impulses in Eqs. (3.21) and (3.22) consist of the first-order (only h_3 term) and the second-order terms of the disorder h_j . The first-order term leads to the ‘‘direct jitter’’ [23] of the solitons, determined by Eq. (3.9). This ‘‘direct jitter’’ is a single-soliton effect and is insensitive to the soliton pattern. On the contrary, the second-order contribution is responsible for the intersoliton interaction mediated

by the radiation, and it is sensitive to the soliton pattern.

So far, we have considered two special polarizations in the two-soliton evolution: parallel and orthogonal polarizations. In both cases, the jitter of the intersoliton separation occurs, and the fluctuation δy possesses Gaussian statistics. However, the mean square $\langle(\delta y)^2\rangle$ has, in accordance with Eqs. (4.9) and (4.21), essentially different z dependence. For the parallel polarizations $\delta y \sim Dz^{3/2}$, whereas for the orthogonal polarization, $\delta y \sim (Dz)^{1/2}$. An explanation is that the direct jitter is canceled in the parallel polarizations whereas the intersoliton interaction is negligible in comparison with the direct jitter in the orthogonal polarization.

In the general case, when the angle between the soliton polarizations does not coincide with 0 or $\pi/2$, or when elliptic polarizations are considered, δy still possesses Gaussian statistics (at large z). However, both the first- and the second-order terms appear in the forces and impulses. As a result, there are two different contributions, $\sim Dz$ and $\sim D^2z^3$, to $\langle(\delta y)^2\rangle$, related to the direct jitter and to the soliton interaction, respectively. Therefore, a new scale $D^{-1/2}$ has to be introduced. If $z \lesssim D^{-1/2}$ then the first-order term (direct jitter) becomes dominant and $\delta y \sim (Dz)^{1/2}$. If $z \gtrsim D^{-1/2}$ then the second-order terms (interaction) prevail and $\delta y \sim Dz^{3/2}$. Unfortunately, it is a difficult task to find coefficients in the general case. Nevertheless, the estimates fix the z dependence of the typical fluctuation of the intersoliton separation and determine its value for arbitrary polarizations.

V. NUMERICAL SIMULATIONS

In this section, we discuss the results of the direct numerical simulations based on Eq. (2.2) which have been performed for the one- and two-soliton patterns. The initial conditions are the perfect solitons determined by Eq. (2.6) (with the linear polarization), and the statistics of the disorder is determined by Eqs. (2.3) and (2.4). Recall that Eqs. (2.2) and (2.6) are written in terms of the dimensionless units when the Kerr nonlinearity, chromatic dispersion, and soliton width are rescaled to unities.

Since we aim to observe the soliton behavior in the long haul transmission, the major obstacles in the computation result from the long time integration. As we have observed, the perturbed solitons shed radiation and the radiation moves away from the solitons. In the computational domain, which is finite, the radiation interacts eventually with the artificial boundaries (experiencing a reflection), and this causes spurious numerical results. In order to overcome these undesirable numerical artifacts we implement the so-called transparent boundary conditions. We refer the reader to Ref. [26] for more details about these boundary conditions.

Utilizing the Runge-Kutta method supplemented by the transparent boundary conditions, we first investigate the single-soliton case and then the interaction of two solitons in two different polarization cases. Specifically, we examine the degradation law in the single-soliton case and the statistics of the intersoliton interaction. The results are presented in Figs. 1–3. Figure 1 is for the single-soliton case, and Figs. 2 and 3 correspond to the two-soliton case.

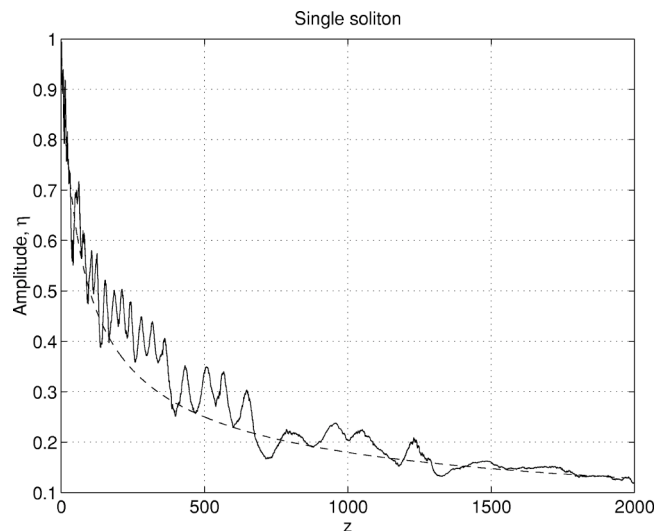


FIG. 1. Soliton amplitude as a function of the position along the fiber. The solid curve gives the numerical result for a realization of the disorder. The dashed curve represents the theoretical prediction.

Figure 1 shows a dependence of the soliton amplitude on the propagation length z for a realization of the disorder h_j , generated in accordance with Eqs. (2.3) and (2.4) where $D = 0.0225$ was chosen. This choice is made to have a possibility to compare the numerical results with the theoretical predictions in a wide range of the soliton amplitude. The solid and dashed curves represent the computational result for a representative realization of the disorder and the analytical prediction from Eq. (3.20), respectively.

Now we turn to the two-soliton case. In Fig. 2, we plot the mean square soliton separation fluctuation $\langle(\delta y)^2\rangle$ as a function of the propagation length z in the case of the parallel polarization. Here, we take the noise intensity $D = 0.0125^2$

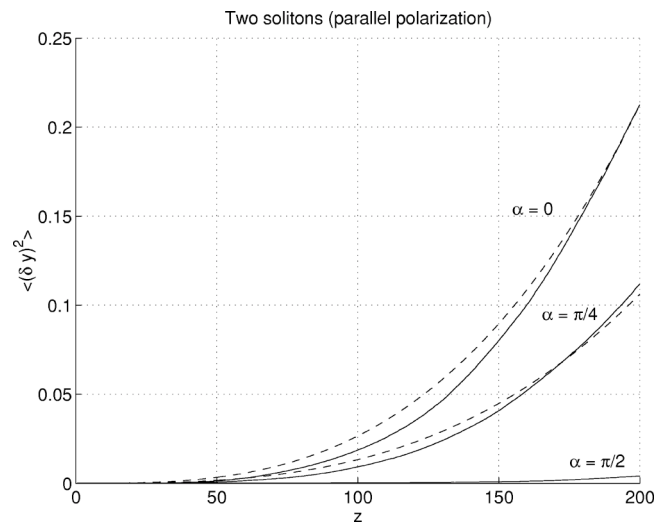


FIG. 2. Parallel polarization case: mean square of the intersoliton separation $\langle(\delta y)^2\rangle$ as a function of the position along the fiber. The phase mismatches are $\alpha = 0$, $\pi/4$, and $\pi/2$. The dashed curves correspond to the theoretical prediction (4.9) and the solid ones are obtained as a result of averaging over 40 realizations of the disorder.

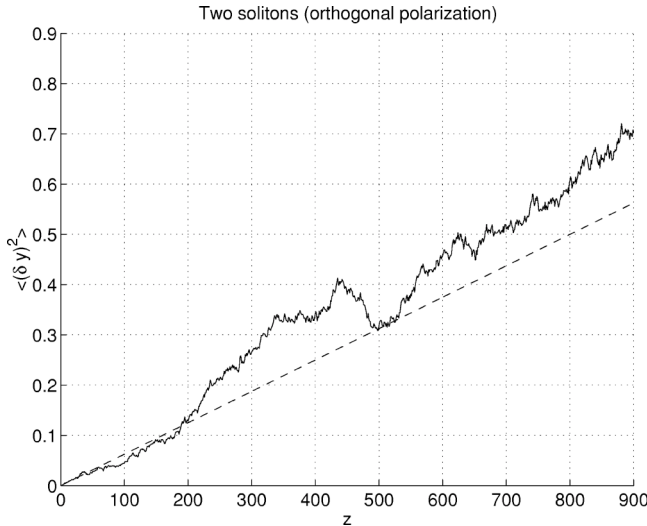


FIG. 3. Orthogonal polarization case: mean square of the intersoliton separation $\langle(\delta y)^2$ as a function of the position along the fiber. The dashed curve corresponds to the theoretical prediction and the solid one is obtained as a result of averaging over 40 realizations of the disorder.

which is much smaller than in the single-soliton case. This is because we need to observe the intersoliton dynamics in the region where the soliton does not lose its energy significantly. The initial distance between the solitons, y_0 , needs to be large enough to avoid the direct interaction between solitons. In this simulation, we take $y_0=20$. Each soliton position is measured as reported in Ref. [26]. For the sake of comparison, three different phase mismatches $\alpha=0, \pi/4, \pi/2$ are examined. For each α , we average the fluctuations $(\delta y)^2$ over 40 realizations of the disorder. The solid curves in Fig. 2 represent the numerical results for $\langle(\delta y)^2$ and the dashed curves stand for the theoretical predictions (4.9).

In Fig. 3, we plot the mean square soliton separation fluctuation $\langle(\delta y)^2$ as a function of the propagation length z in the case of the orthogonal polarization. We take the same noise intensity $D=0.0125^2$ and the same initial separation $y_0=20$ as for the parallel polarizations. Each soliton position is measured as reported in Ref. [26]. The solid curve in Fig. 3 represents the numerical result for $\langle(\delta y)^2$ (averaged over 40 realizations of the disorder) and the dashed line stands for the theoretical prediction (4.21).

All the figures demonstrate a reasonable agreement between the theory and the numerics. Thus, our theoretical predictions are confirmed by the results obtained from the direct numerical simulation of Eq. (2.2) with the initial conditions for the single- and two-soliton cases.

VI. CONCLUSION

Let us summarize our major results concerning the role of radiation (continuous spectrum) in the soliton (nonlinear) mode of the optical signal propagation through a fiber with randomly varying birefringence (leading to the PMD effect).

The major effect reported in this paper is an emergence of the interaction between solitons, mediated by the radiation

shed by the solitons due to the disorder. This gives rise to random displacements of the solitons, which are Gaussian random variables with zero average. The jitter is independent of the soliton separation, which is due to one-dimensional nature of the fiber. The negligible systematic drift is explained by the reflectiveness character of the radiation scattering on solitons in the integrable Manakov equation. This effect is in contrast to the nonintegrable case investigated in Ref. [31]. The results we presented in this paper are similar to ones obtained in the paper [26] for the chromatic dispersion disorder, although the theoretical analysis for the PMD disorder is more complex.

We demonstrated that due to the PMD disorder, soliton loses its energy to radiation during propagation. The amplitude decays by the order of its initial value, at the distance $z \sim 1/D$ (in our dimensionless units when the Kerr nonlinearity, chromatic dispersion, and soliton width are rescaled to unities) where D is the strength of the disorder fluctuations (which is assumed to be weak: $D \ll 1$). Note that in the region of strong degradation, the PMD disorder leads to faster degradation of the soliton than the chromatic dispersion disorder examined in Ref. [26] (the asymptotic laws for the soliton amplitude are $\propto z^{-1/2}$ and $\propto z^{-1/4}$, respectively). We also established the profile of radiation emitted by the soliton. The soliton degradation is negligible (it is a necessary condition for the successful information transmission) at $Dz \ll 1$. Nevertheless, even for small Dz , the soliton interaction caused by radiation can be an essential source of the information losses.

In addition to the soliton interaction there is a phenomenon called direct jitter of the solitons [23] which is a single-soliton effect, described by Eq. (3.9). If all the solitons have the same polarization then the direct jitter causes identical displacements of the solitons. Then an influence of the jitter on the detection of the information can be removed by a simple compensation scheme known as “setting the clock.” For different polarizations, however, the direct jitter can lead to significant information losses.

We examined in detail the evolution of two solitons propagating in the same frequency channel. The soliton interaction appears to be suppressed for the orthogonal polarizations when the direct jitter dominates. For the parallel polarizations, the direct jitter does not influence the soliton separation and its fluctuations δy are determined by the soliton interaction, giving $\delta y \sim Dz^{3/2}$. Note a remarkable phase dependence of the soliton interaction [see Eq. (4.9)], having a deep minimum at the phase mismatch $\alpha=\pi/2$. Generally, for arbitrary polarizations, both the direct jitter and the soliton interaction contribute to the fluctuations of the soliton separation, prevailing at different z . At $z \lesssim D^{-1/2}$ the direct jitter dominates, whereas at $z \gtrsim D^{-1/2}$ the intersoliton interaction is the major effect.

We performed extensive direct numerical simulations for the single- and two-soliton patterns, which confirm our theoretical predictions. The results of the simulations and their comparison with the theory are presented in Figs. 1–3, which demonstrate reasonable agreements between the numerics and the theory.

Considering multisoliton case, we can treat radiation (delocalized modes) as a superposition of contributions related

to each soliton. The reflectiveness character of the radiation scattering on solitons, noted above, essentially simplifies the analysis, since the radiation emitted by a soliton monotonically spreads in both directions. This enables one to estimate “forces,” caused by the radiation, in the multisoliton pattern via the forces obtained from the two-soliton case. The dispersion of the displacements induced by the intersoliton interaction increases as the number of solitons N grows in the fiber. In this case, the dispersion is proportional to $N^{1/2}$, where N is the number of the solitons involved in the interaction. Since the number N is proportional to z (at a given average density of solitons in the pattern) we reach the proportionality law $\delta y \propto z^2$.

Now we discuss our results in connection with the soliton mode of the information transmission. We established that the intersoliton interaction becomes the most dangerous source of the information losses overcoming the direct jitter. Because of the dependence $\delta y \propto z^2$ the soliton interaction can be more essential than the Elgin-Gordon-Haus effect [27,28]. We established that in the two-soliton case the interaction is suppressed for the orthogonal polarizations and for the phase mismatch $\alpha = \pi/2$ in the case of parallel polarization. One can take advantage of these properties to reduce the soliton displacements and consequently, to minimize the information loss. In the real information transmission systems, however, long sequences of solitons are used as information carriers. In this case, not all soliton pairs can achieve the mutual orthogonal polarization or the phase mismatch $\alpha = \pi/2$. Therefore, the random jitter caused by the soliton interaction due to the PMD disorder can be the most essential error source in the high-rate information transmission systems.

ACKNOWLEDGMENTS

We are grateful to M. Chertkov, I Gabitov, and I. Kolokolov for valuable comments and useful discussions.

APPENDIX A: KAUP PERTURBATION TECHNIQUE

Here we present some technical details necessary for a consistent derivation of the results formulated in the main body of the paper.

1. Eigenfunctions of operator \hat{L}_1

Let us recall some of the well-known properties in the perturbation near a single-soliton solution described by the nonlinear Schrödinger equation [30]

$$-i\partial_z\Psi = \partial_t^2\Psi + 2|\Psi|^2\Psi. \quad (\text{A1})$$

We expand Ψ near the single-soliton solution $\Psi_{sol} = \exp(i\alpha + iz)\cosh^{-1}(t)$. Then, one can write Ψ as

$$\Psi = [\cosh^{-1}(t) + v]\exp[iz + i\alpha].$$

Using the above expression and Eq. (A1), we find

$$i\partial_z\begin{pmatrix} v \\ v^* \end{pmatrix} + \hat{L}_1\begin{pmatrix} v \\ v^* \end{pmatrix} = 0. \quad (\text{A2})$$

Here the operator \hat{L}_1 is

$$\hat{L}_1 = (\partial_t^2 - 1)\hat{\sigma}_3 + \frac{2}{\cosh^2(t)}(2\hat{\sigma}_3 + i\hat{\sigma}_2). \quad (\text{A3})$$

Evidently,

$$\hat{L}_1^* = \hat{L}_1, \quad \hat{\sigma}_1\hat{L}_1\hat{\sigma}_1 = -\hat{L}_1, \quad \hat{L}_1^T = \hat{\sigma}_3\hat{L}_1\hat{\sigma}_3. \quad (\text{A4})$$

The spectrum of the linear operator is determined by the equation $\hat{L}_1 f = \lambda f$. A general solution of this equation reads

$$f_k = \exp[ikt] \left\{ 1 - \frac{2ik \exp(-t)}{(k+i)^2 \cosh(t)} \right\} \begin{pmatrix} 0 \\ 1 \end{pmatrix} + \frac{\exp(ikt)}{(k+i)^2 \cosh^2(t)} \begin{pmatrix} 1 \\ 1 \end{pmatrix}, \quad \lambda_k = k^2 + 1, \quad (\text{A5})$$

where k runs from $-\infty$ to $+\infty$. Due to the property (A4), the functions $\bar{f}_k = \hat{\sigma}_1 f_k^*$ are also eigenfunctions of \hat{L}_1 :

$$\bar{f}_k = \exp[-ikt] \left\{ 1 + \frac{2ik \exp(-t)}{(k-i)^2 \cosh(t)} \right\} \begin{pmatrix} 1 \\ 0 \end{pmatrix} + \frac{\exp(-ikt)}{(k-i)^2 \cosh^2(t)} \begin{pmatrix} 1 \\ 1 \end{pmatrix}, \quad \lambda_k = -(k^2 + 1). \quad (\text{A6})$$

There are also bound states corresponding to marginally stable modes:

$$f_0 = \frac{1}{\cosh(t)} \begin{pmatrix} 1 \\ -1 \end{pmatrix}, \quad \lambda_0 = 0,$$

$$f_1 = \begin{pmatrix} 1 \\ 1 \end{pmatrix} \frac{\tanh(t)}{\cosh(t)}, \quad \lambda_1 = 0. \quad (\text{A7})$$

Double poles at $k = \pm i$ mean that two more functions must be added for closure, namely,

$$f_2 = \frac{t}{\cosh(t)} \begin{pmatrix} 1 \\ -1 \end{pmatrix}, \quad \hat{L}_1 f_2 = -2f_1, \quad (\text{A8})$$

$$f_3 = \frac{t \tanh(t) - 1}{\cosh(t)} \begin{pmatrix} 1 \\ 1 \end{pmatrix}, \quad \hat{L}_1 f_3 = -2f_0. \quad (\text{A9})$$

Note that due to the property (A4), the left eigenfunctions of the operator \hat{L}_1 can be written as $f_k^+ \hat{\sigma}_3, \bar{f}_k^+ \hat{\sigma}_3$. This leads to a set of orthogonality conditions for the eigenfunctions. In an explicit form, the conditions can be written as

$$\int_{-\infty}^{+\infty} dt \bar{f}_k^+ \hat{\sigma}_3 f_q^- = 2\pi\delta(k-q), \quad \int_{-\infty}^{+\infty} dt f_k^+ \hat{\sigma}_3 f_q^- = -2\pi\delta(k-q), \quad (\text{A10})$$

$$\int_{-\infty}^{+\infty} dt f_2^+ \hat{\sigma}_3 f_1 = 2, \quad \int_{-\infty}^{+\infty} dt f_0^+ \hat{\sigma}_3 f_3 = -2. \quad (\text{A11})$$

2. Eigenfunctions of operator \hat{L}_2

We now present eigenfunctions of the operator (3.5). The set contains functions of the continuous spectrum $\varphi_k, \bar{\varphi}_k$, satisfying

$$\hat{L}_2 \varphi_k = (k^2 + 1) \varphi_k, \quad \hat{L}_2 \bar{\varphi}_k = -(k^2 + 1) \bar{\varphi}_k. \quad (\text{A12})$$

Evidently,

$$\hat{L}_2^* = \hat{L}_2, \quad \hat{\sigma}_1 \hat{L}_2 \hat{\sigma}_1 = -\hat{L}_2, \quad \hat{L}_2^+ = \hat{\sigma}_3 \hat{L}_2 \hat{\sigma}_3. \quad (\text{A13})$$

Therefore,

$$\bar{\varphi}_k = \hat{\sigma}_1 \varphi_k^*, \quad \bar{\varphi}_{-k} = \hat{\sigma}_1 \varphi_{-k}^*. \quad (\text{A14})$$

There are also localized eigenfunctions which are zero modes of \hat{L}_2 , satisfying $\hat{L}_2 \varphi_{0,2} = 0$.

The eigenfunctions corresponding to the continuous spectrum are

$$\varphi_k = \begin{pmatrix} 0 \\ 1 \end{pmatrix} \tilde{\Psi}_k, \quad \bar{\varphi}_k = \begin{pmatrix} 1 \\ 0 \end{pmatrix} \tilde{\Psi}_{-k}, \quad (\text{A15})$$

$$\tilde{\Psi}_k = \frac{k+i \tanh t}{k+i} e^{ikt}. \quad (\text{A16})$$

We obtain the following orthogonality conditions:

$$\int_{-\infty}^{+\infty} dt \bar{\varphi}_k^+ \hat{\sigma}_3 \bar{\varphi}_q = 2\pi \delta(k-q),$$

$$\int_{-\infty}^{+\infty} dt \varphi_k^+ \hat{\sigma}_3 \varphi_q = -2\pi \delta(k-q), \quad (\text{A17})$$

analogous to Eq. (A10). The zero modes of the operator (3.3) can be written as

$$\varphi_0(t) = \begin{pmatrix} 1 \\ 1 \end{pmatrix} \cosh^{-1} t, \quad \varphi_2(t) = \begin{pmatrix} 1 \\ -1 \end{pmatrix} \cosh^{-1} t. \quad (\text{A18})$$

They are normalized according to

$$\int_{-\infty}^{+\infty} dt \varphi_0^T \hat{\sigma}_3 \varphi_2 = 4. \quad (\text{A19})$$

APPENDIX B: FORCE AND IMPULSE FOR PARALLEL POLARIZATION

Using Eq. (4.4) and taking φ_k near y_1 from Eq. (4.3), one can derive

$$\mathcal{F}_{vv}(z) = 2 \int \frac{dq dk}{(2\pi)^2} a_{k\parallel} a_{q\parallel}^* \int dx \frac{\tanh x}{\cosh^2 x} \times \frac{(k+i \tanh x)(q-i \tanh x)}{(k+i)(q-i)} e^{ikx-iqx}, \quad (\text{B1})$$

$$\mathcal{F}_{vh}(z) = -\text{Im} \left\{ H(z) \int \frac{dk}{2\pi} a_{k\parallel}^* \int dx \frac{\sinh^2 x - 1}{\cosh^3 x} \times \frac{k-i \tanh x}{k-i} e^{-ikx} \right\}. \quad (\text{B2})$$

Integrating over x and plugging Eq. (4.5) into the above equations, we find

$$\mathcal{F}_{vv}(z) = \frac{i\pi}{2^6} \int \frac{dq dk (k^2 - q^2)^2}{\sinh[\pi(k-q)/2] \cosh[\pi k/2] \cosh[\pi q/2]} \times \left[\frac{k-i}{k+i} e^{-i\alpha-iky} + \frac{q+i}{q-i} e^{i\alpha+iqy} + \frac{k-i}{k+i} \frac{q+i}{q-i} e^{i(q-k)y} \right] \times \int_0^z dz_1 dz_2 H^*(z_1) H(z_2) e^{i(k^2+1)(z-z_1)} e^{-i(q^2+1)(z-z_2)}, \quad (\text{B3})$$

$$\mathcal{F}_{vh} = \frac{\pi}{8} \text{Re} \left\{ \int dk \frac{k(k^2+1)}{\cosh^2(\pi k/2)} \left[\frac{k+i}{k-i} e^{iky+i\alpha} \right] H^*(z) \times \int_0^z dz_1 H(z_1) e^{-i(k^2+1)(z-z_1)} \right\}. \quad (\text{B4})$$

For the sake of convenience, we rewrite the force F_{vv} as $\partial_z P - (1/3)\Lambda$, where

$$P = \frac{\pi}{2^6} \int \frac{dq dk (k^2 - q^2)}{\sinh[\pi(k-q)/2] \cosh[\pi k/2] \cosh[\pi q/2]} \times \left[\frac{k-i}{k+i} e^{-i\alpha-iky} + \frac{q+i}{q-i} e^{i\alpha+iqy} + \frac{k-i}{k+i} \frac{q+i}{q-i} e^{i(q-k)y} \right] \times \int_0^z dz_1 dz_2 H^*(z_1) H(z_2) e^{i(k^2+1)(z-z_1)-i(q^2+1)(z-z_2)}, \quad (\text{B5})$$

and, with an exponential accuracy,

To obtain Eq. (B6), one has to take the integral over k and q omitting exponentially small terms. As it follows from Eqs. (3.24) and (3.27), the structure of \mathcal{P}_{vh} is similar to one of the forces, \mathcal{F}_{vh} . Integrating over x , we find

$$\mathcal{P}_{vh} = \frac{-\pi^2}{16} \text{Im} \left\{ \int dk \frac{(k^2+1) \tanh(\pi k/2)}{\cosh^2(\pi k/2)} \left[\frac{k+i}{k-i} e^{iky+i\alpha} \right] \times H^*(z) \int_0^z dz_1 H(z_1) e^{-i(k^2+1)(z-z_1)} \right\}. \quad (\text{B7})$$

Thus, one can rewrite Eqs. (3.21) and (3.22) as

$$\mathcal{F} = \mathcal{F}_{vh} + \mathcal{F}_{vv} = \partial_z P + \Lambda,$$

$$\partial_{zy} = h_3 + \mathcal{P}, \quad \mathcal{P} = 2P + 2 \int_0^z dz' \Lambda(z') + \mathcal{P}_{vh}. \quad (\text{B8})$$

1. Average force and impulse

Let us find the average of the force, $\langle \mathcal{F} \rangle$, over the disorder. Using Eq. (B3) we obtain

$$\begin{aligned} \langle \mathcal{F}_{vv} \rangle &= \frac{iD}{2^5} \int \frac{dq dk (k^2 - q^2)^2}{\sinh[\pi(k-q)/2] \cosh[\pi k/2] \cosh[\pi q/2]} \\ &\times \left[\frac{k-i}{k+i} e^{-i\alpha -iky} + \frac{q+i}{q-i} e^{i\alpha +iqy} + \frac{k-i}{k+i} \frac{q+i}{q-i} e^{i(q-k)y} \right] \\ &\times \frac{i\pi(1 - e^{i(k^2 - q^2)z})}{k^2 - q^2}. \end{aligned} \quad (\text{B9})$$

We take an integration contour surrounding poles, which are not on the real axis. Then, we find that \mathcal{F}_{vv} is exponentially small. Similarly, the average of the force \mathcal{F}_{vh} is also negligible, and hence, the average of overall force \mathcal{F} in this approximation is zero.

Now let us calculate the average of the impulse \mathcal{P} . Notice that, due to Eqs. (B4) and (B7), the averages of both Λ and \mathcal{P}_{vh} are negligible, $\propto \exp(-\text{const} \times y)$ at any z . Introducing new variables $p_{\pm} = k \pm q$, one obtains

$$\begin{aligned} \langle P(z) \rangle &= \frac{\pi D}{2^6} \int \frac{dp_+ dp_-}{\cosh[\pi k/2] \cosh[\pi q/2]} \\ &\times \left[\frac{k-i}{k+i} e^{-i\alpha -iy(p_+ + p_-)/2} + \frac{q+i}{q-i} e^{i\alpha +iy(p_+ - p_-)/2} \right. \\ &\left. + \frac{k-i}{k+i} \frac{q+i}{q-i} e^{-ip_-y} \right] \frac{i(1 - e^{ip_+z})}{\sinh[\pi p_-/2]}. \end{aligned} \quad (\text{B10})$$

The main contribution to the above integral is originated at small values of p_- . Since α -dependent terms are exponentially small in y , we find that at large z , $z \gg y$, the average value of the total impulse is

$$\langle P(z) \rangle = \frac{\pi D}{2^4} \int \frac{dp}{\cosh^2(\pi p/4)} = \frac{D}{4}. \quad (\text{B11})$$

2. Impulse fluctuations

Now we calculate the impulse fluctuation $\langle\langle \mathcal{P}^2 \rangle\rangle = \langle \mathcal{P}^2 \rangle - \langle \mathcal{P} \rangle \langle \mathcal{P} \rangle$. First let us obtain the main contribution, coming from Λ term in Eq. (B8). Using the relation (B4) and taking \mathcal{F}_{vh} from Eq. (B6), we find

$$\begin{aligned} \langle\langle \Lambda(z_1) \Lambda(z_2) \rangle\rangle &= \frac{\pi^2}{64} \left\langle \left\langle \text{Re} \left[H(z_1) \int dk \frac{k(k^2 + 1)}{\cosh^2(\pi k/2)} \right. \right. \right. \\ &\times \frac{k+i}{k-i} e^{iky+i\alpha} \int_0^{z_1} dz'_1 H(z'_1) e^{-i(k^2+1)(z_1-z'_1)} \left. \right. \\ &\times \text{Re} \left[H^*(z_2) \int dq \frac{q(q^2 + 1)}{\cosh^2(\pi q/2)} \frac{q-i}{q+i} e^{-iqy-i\alpha} \right. \\ &\times \left. \left. \left. \int_0^{z_2} dz'_2 H^*(z'_2) e^{i(q^2+1)(z_2-z'_2)} \right] \right] \right\rangle. \end{aligned} \quad (\text{B12})$$

The terms proportional to $\langle HH \rangle \langle H^* H^* \rangle$ vanish due to the relation (3.7). The remaining term is

$$\begin{aligned} \frac{\pi^2}{64} \delta(z_1 - z_2) D^2 \text{Re} \left[\int dp_+ dp_- \frac{kq(k^2 + 1)(q^2 + 1)}{\cosh^2(\pi k/2) \cosh^2(\pi q/2)} \right. \\ \left. \times \frac{k+i}{k-i} \frac{q-i}{q+i} (-i) e^{ip_-y} \frac{1 - e^{-ip_+z}}{p_+ p_-} \right], \end{aligned} \quad (\text{B13})$$

where $(p_{\pm} = k \pm q)$. The major contribution is formed at small p_+ , $p_- \sim 1/y$, and we find

$$\begin{aligned} \langle\langle \Lambda(z_1) \Lambda(z_2) \rangle\rangle &= \frac{\pi^3}{32} \delta(z_1 - z_2) D^2 \int_0^{\infty} dp \frac{p(p^2 + 1)^2}{\cosh^4(\pi p/2)} \\ &= 0.204 D^2 \delta(z_1 - z_2). \end{aligned} \quad (\text{B14})$$

The fluctuation of the differences between forces acting on two solitons has an additional factor $2[1 + \cos(2\alpha)]$, and we find

$$\begin{aligned} 4 \left\langle \left\langle \int_0^{z_1} dz'_1 [\Lambda^{(2)}(z'_1) - \Lambda^{(1)}(z'_1)] \right. \right. \\ \left. \left. \times \int_0^{z_2} dz'_2 [\Lambda^{(2)}(z'_2) - \Lambda^{(1)}(z'_2)] \right\rangle \right\rangle \\ = 8G_{\parallel} [1 + \cos(2\alpha)] D^2 z, \end{aligned} \quad (\text{B15})$$

where the superscripts 1 and 2 denote the first and the second solitons, respectively, and $z = \min(z_1, z_2)$. Here G_{\parallel} is a numerical factor, $G_{\parallel} = 0.204$.

Now we evaluate additional contribution to the fluctuations of the impulse and position. First we examine the impulse P . Using Eq. (B5), we find

$$\begin{aligned} \langle\langle P(z_1) P(z_2) \rangle\rangle &= - \frac{\pi^2 D^2}{2^{12}} \int \frac{dk_+ dk_- dq_+ dq_- (k_1^2 - q_1^2)(k_2^2 - q_2^2) e^{i(q_2^2 - k_2^2)\zeta}}{\sinh \frac{\pi(k_1 - q_1)}{2} \sinh \frac{\pi(k_2 - q_2)}{2} \cosh \frac{\pi k_1}{2} \cosh \frac{\pi k_2}{2} \cosh \frac{\pi q_1}{2} \cosh \frac{\pi q_2}{2}} \\ &\times \left[\frac{k_1+i}{k_1-i} e^{i\alpha+iq_1y} + \frac{q_1-i}{q_1+i} e^{-i\alpha-ik_1y} + \frac{k_1+i}{k_1-i} \frac{q_1-i}{q_1+i} \right] \left[\frac{k_2+i}{k_2-i} e^{i\alpha+iq_2y} + \frac{q_2-i}{q_2+i} e^{-i\alpha-ik_2y} + \frac{k_2+i}{k_2-i} \frac{q_2-i}{q_2+i} \right] \\ &\times \frac{e^{ik_-y+iq_+y} (1 - e^{-ik_+k_-z}) (1 - e^{-iq_+q_-z})}{k_+ k_- q_+ q_-}, \end{aligned} \quad (\text{B16})$$

where $k_{\pm} = k_1 \pm q_2$, $q_{\pm} = k_2 \pm q_1$, $z = \min(z_1, z_2)$, and $\zeta = |z_1 - z_2|$. Again, the terms proportional to $\langle HH \rangle \langle H^* H^* \rangle$ vanish.

We now let $\zeta=0$ and calculate the simultaneous correlation and consider α -independent contributions to the fluctuation. One of the contributions comes from α -independent terms in the square brackets of Eq. (B16). The main contribution to the above integral is formed at $k_-, q_- \sim 1/y$, and hence, one obtains

$$\langle\langle P^2 \rangle\rangle_1 = \frac{\pi^4 D^2}{2^{14}} \int_{y/z}^{\infty} \frac{dk_+ dq_+ (k_+^2 - q_+^2)^2}{\cosh^2[\pi k_+/4] \cosh^2[\pi q_+/4] k_+ q_+ \sinh^2[\pi(k_+ - q_+)/4]} \cdot \quad (B17)$$

The other contribution comes from α -dependent terms in the square brackets of Eq. (B16). This consists of two equal parts, which are different from the previous contribution by the absence of one out of two oscillating factors in q_- (or k_-). Integrating over k_- , we find

$$\begin{aligned} \langle\langle P^2 \rangle\rangle_2 &= \frac{\pi^4 D^2}{2^9} \int_{y/z}^{\infty} \frac{dk_+}{k_+ \cosh^2(\pi k_+/4)} \int \frac{dq_+ dq_-}{2\pi i q_+ q_-} \\ &\times [1 - \exp(-iq_+ q_- z)] \\ &\times \frac{[(k_+/2)^2 - q_1^2][(k_+/2)^2 - k_2^2]}{\cosh \frac{\pi k_2}{2} \cosh \frac{\pi q_1}{2} \sinh \frac{\pi(k_+ - 2q_1)}{4} \sinh \frac{\pi(k_+ - 2k_2)}{4}}. \end{aligned} \quad (B18)$$

$$\begin{aligned} \langle\langle P^2(z) \rangle\rangle &= \frac{\pi^4 D^2}{2^{11}} [\ln z + \ln(z/y) + \cos(\alpha) \ln(z/y^2)] \\ &\times \int_0^{\infty} \frac{dk k^3}{\cosh^2(\pi k/2)} = 0.14 D^2 \left[\ln \frac{z^2}{y} + \cos(\alpha) \ln \frac{z}{y^2} \right]. \end{aligned} \quad (B19)$$

The major contribution to the integral is formed at $k_+ \sim 1$ and small values of q_{\pm} . Now let us find the α -dependent contribution to the fluctuation. The main part originates from the product of α -dependent and α -independent terms in the right-hand side of Eq. (B16). It is proportional to $\cos \alpha$ multiplied by the right-hand side of Eq. (B18) with an extra factor $[(k_2+i)/(k_2-i)] \exp[iy(q_+ + q_-)/2]$ in the integral. Hence, the integration is formed over q_{\pm} , from $q \sim 1$ up to $q \sim 1/y$. We find that additional α -dependent contributions are $\sim 1/y$. Extracting the main contributions which are proportional to $\ln(z/y)$ in Eq. (B17), $\ln(z)$ in Eq. (B18), and $\ln(z/y^2)$ in the α -dependent terms, one finds

It is much smaller than Eq. (B14) at large z .

To obtain the correlation at $\zeta \neq 0$, $\zeta \ll z$, one should take into account that the integral (B16) is formed in the region where one of the variables k_{\pm}, q_{\pm} is $O(1)$ while the others are much smaller than unity. Taking this into account, one derives

$$\begin{aligned} \langle\langle P(z_1) P(z_2) \rangle\rangle &= 0.14 D^2 \left[\ln \frac{z^2}{y} + \cos \alpha \ln \frac{z}{y^2} \right] \\ &\times \int_0^{\infty} \frac{dk k^3}{\cosh^2(\pi k/2)} \cos(k^2 \zeta). \end{aligned} \quad (B20)$$

The correlation vanishes algebraically as $1/\zeta$ and $\int d\zeta \langle\langle P(z) P(z+\zeta) \rangle\rangle \propto 1/y$, which is negligible. At $\zeta \sim z$ one finds that the correlation is $\propto 1/z^2$. This allows us to neglect the contribution from the impulse P to the position fluctuations.

We now turn to the cross correlation. Integrating over z and using Eq. (3.7), we derive

$$\begin{aligned} \langle\langle P(z+\zeta) \Lambda(z) \rangle\rangle &= -\frac{\pi^2 D^2}{2^{10}} \operatorname{Re} \left\{ \int dk_1 dk_2 dq \frac{q(q^2+1)}{\cosh^2 \frac{\pi q}{2}} \frac{(k_1^2 - k_2^2) e^{i(k_1^2 - k_2^2)\zeta}}{\sinh[\pi(k_1 - k_2)/2] \cosh(\pi k_1/2) \cosh(\pi k_2/2)} \right. \\ &\left. \times \frac{k_1 - iq + i i(1 - e^{i(k_1^2 - q^2)z})}{k_1 + iq - i} \frac{e^{-i(k_1 - q)y}}{(k_1^2 - q^2)} \right\}, \end{aligned} \quad (B21)$$

which is nonzero at $\zeta > 0$. Now we extract the main part of the integral forming at small values of $k_1 - q$ and find

$$\langle\langle P(z+\zeta) \Lambda(z) \rangle\rangle = -\frac{\pi^3 D^2}{2^{11}} \operatorname{Re} \left\{ \int dk \int_0^{\infty} dp \frac{(p^2+1)(p^2-k^2) e^{i(p^2-k^2)\zeta}}{\cosh^3 \frac{\pi p}{2} \cosh \frac{\pi k}{2} \sinh \frac{\pi(p-k)}{2}} \right\}. \quad (B22)$$

Then we obtain

$$\langle\langle P(z+\zeta) \int_0^z \Lambda(z_1) dz_1 \rangle\rangle = -\frac{\pi^3 D^2}{2^{10}} \operatorname{Re} \left\{ \int dk \int_0^\infty dp \frac{(p^2+1)e^{i(p^2-k^2)\zeta}}{\cosh^3(\pi p/2) \cosh(\pi k/2)} \frac{i(1-e^{i(p^2-k^2)z})}{\sinh[\pi(p-k)/2]} \right\}. \quad (\text{B23})$$

The simultaneous correlation, i.e., the correlation at $\zeta=0$, is

$$-\frac{\pi^4 D^2}{2^{10}} \int_0^\infty \frac{dp_+(p_+^2/4+1)}{\cosh^4(\pi p_+/2)} \approx -0.090 D^2. \quad (\text{B24})$$

Thus, the cross correlation is negligible.

Let us discuss remaining contributions to the impulse fluctuations. The pair correlation function of the extra impulse \mathcal{P}_{vh} is $\approx 0.78 D^2 \delta(z_1 - z_2)$, similar to Eq. (B14). The corresponding contribution to the position fluctuation is $\propto D^2 z$ and can be omitted. Its cross correlation with Λ is small because we take imaginary part in Eq. (3.24) and real part in Eq. (3.24). This distinction leads to an expression analogous to Eq. (B13) but with imaginary part of the integral, which is negligible. The simultaneous cross correlation between \mathcal{P}_{vh} and P is similar to Eq. (B21) with an extra factor $-(\pi/2q) \tanh(\pi q/2)$ in the integrand and taking the imaginary part of the integral instead of the real part. Then, we find that it is negligible in comparison with Eq. (B24). Summarizing the results obtained so far and using Eq. (B14), we find Eq. (4.6).

APPENDIX C: FORCE AND IMPULSE IN ORTHOGONAL POLARIZATION CASE

In this case, we have only the force Φ_{vv} and the extra impulse \mathcal{P}_{vv} nonzero. Therefore, Eqs. (3.21) and (3.22) are reduced to

$$\frac{d}{dz} \beta_1 = \Phi_{vv}, \quad \frac{d}{dz} y_1 = h_3 + 2\beta_1 + \mathcal{P}_{vv}. \quad (\text{C1})$$

First we examine the force. We represent $\Phi_{vv} = \Phi_0 + \Phi_1 + \Phi_1^*$, where Φ_0 and Φ_1 contain the field H only in the form of H^*H and HH , respectively. Then, one can find, using Eqs. (4.13) and (4.15),

$$\begin{aligned} \Phi_0 &= \int dx \frac{\tanh x}{\cosh^2 x} \int \frac{dq dk}{(2\pi)^2} \frac{e^{ikx-iqx} a_{k\perp} a_{q\perp}^*}{(k+i)^2 (q-i)^2} \\ &\times \left\{ \frac{2[(q-i \tanh x)^2 + (k+i \tanh x)^2]}{\cosh^2 x} + 4 \cosh^{-4} x + 4(q - i \tanh x)^2 (k+i \tanh x)^2 \right\}, \end{aligned} \quad (\text{C2})$$

$$\begin{aligned} \Phi_1 &= \int dx \frac{\tanh x}{\cosh^2 x} \int \frac{dq dk}{(2\pi)^2} \frac{e^{ikx+iqx} a_{k\perp} a_{q\perp}}{(k+i)^2 (q+i)^2} \left\{ \frac{1}{\cosh^4 x} \right. \\ &+ \frac{4}{\cosh^2 x} \left[(q+i)^2 - 2iq \frac{e^{-x}}{\cosh x} + \frac{1}{\cosh^2 x} \right] + \left[(k+i)^2 \right. \\ &\left. \left. - 2ik \frac{e^{-x}}{\cosh x} + \frac{1}{\cosh^2 x} \right] \right\} \frac{e^{-x}}{\cosh x} \left[(q+i)^2 - 2iq \frac{e^{-x}}{\cosh x} \right] \end{aligned}$$

$$\left. + \frac{1}{\cosh^2 x} \right\}. \quad (\text{C3})$$

Integration over x leads to

$$\Phi_0 = \int \frac{dk dq}{24\pi} \frac{ia_{k\perp} a_{q\perp}^* (k^2 - q^2)^2 (1 + k^2 + kq + q^2)}{(k+i)^2 (q-i)^2 \sinh[\pi(k-q)/2]}, \quad (\text{C4})$$

$$\Phi_1 = \int \frac{dk dq}{48\pi} \frac{ia_{k\perp} a_{q\perp} (k+q)^2 (1 + k^2 + q^2 - kq)}{(k+i)^2 (q+i)^2 \sinh[\pi(k+q)/2]} (2 + k^2 + q^2). \quad (\text{C5})$$

Substituting here the expression (4.18), we obtain

$$\begin{aligned} \Phi_0 &= \frac{\pi i}{3 \times 2^5} \int \frac{dk dq (k^2 - q^2)^2 (1 + k^2 + q^2 + kq)}{\cosh[\pi k/2] \cosh[\pi q/2] \sinh[\pi(k-q)/2]} \\ &\times \int_0^z dz_1 dz_2 H(z_1) H^*(z_2) e^{i(k^2+1)(z-z_1) - i(q^2+1)(z-z_2)} \\ &\times \frac{k-i}{(k+i)^2} \frac{q+i}{(q-i)^2} e^{i(q-k)y}, \end{aligned} \quad (\text{C6})$$

$$\begin{aligned} \Phi_1 &= \frac{-\pi i}{3 \times 2^6} \int \frac{dk dq (k+q)^2 (1 + k^2 + q^2 - kq) (2 + k^2 + q^2)}{\cosh(\pi k/2) \cosh(\pi q/2) \sinh[\pi(k+q)/2]} \\ &\times \int_0^z dz_1 dz_2 H(z_1) H^*(z_2) e^{i(k^2+1)(z-z_1) - i(q^2+1)(z-z_2)} \\ &\times \frac{k-i}{(k+i)^2} \frac{q-i}{(q+i)^2} e^{-i(q+k)y - 2i\alpha}. \end{aligned} \quad (\text{C7})$$

Taking integral and omitting exponentially small terms we find

$$\int_0^z dz' \Phi_{vv}(z') = P_0 + P_1 + P_1^*, \quad (\text{C8})$$

$$\begin{aligned} P_0 &= \frac{\pi}{3 \times 2^5} \int \frac{dk dq (k^2 - q^2)^2 (1 + k^2 + q^2 + kq)}{\cosh[\pi k/2] \cosh[\pi q/2] \sinh[\pi(k-q)/2]} \\ &\times \int_0^z dz_1 dz_2 H(z_1) H^*(z_2) e^{i(k^2+1)(z-z_1) - i(q^2+1)(z-z_2)} \\ &\times \frac{k-i}{(k+i)^2} \frac{q+i}{(q-i)^2} e^{i(q-k)y}, \end{aligned} \quad (\text{C9})$$

$$P_1 = \frac{\pi}{3 \times 2^6} \int \frac{dk dq (k+q)^2 (1+k^2+q^2-kq)}{\cosh(\pi k/2) \cosh(\pi q/2) \sinh[\pi(k+q)/2]} \\ \times \int_0^z dz_1 dz_2 H(z_1) H(z_2) e^{i(k^2+1)(z-z_1)-i(q^2+1)(z-z_2)} \\ \times \frac{k-i}{(k+i)^2} \frac{q-i}{(q+i)^2} e^{-i(q+k)y-2i\alpha}. \quad (\text{C10})$$

The extra impulse \mathcal{P}_{vv} can be represented as

$$\mathcal{P}_{vv} = \int \frac{dk dq}{24\pi} \frac{a_{k\perp}^* a_{q\perp} (k+q)(k-q)^2}{(k-i)^2 (q+i)^2 \sinh[\pi(k-q)/2]} \\ \times \left\{ 4(q-k) + \pi[(k-q)^2 + 4] \coth \frac{\pi(k-q)}{2} \right\}. \quad (\text{C11})$$

Thus, in the orthogonal polarization case, we can rewrite Eq. (3.22) as

$$\frac{d}{dz} y = h_3 + \mathcal{P} = h_3 + 2P_0 + 4 \operatorname{Re}(P_1) + \mathcal{P}_{vv}. \quad (\text{C12})$$

1. Average impulse

As it follows from Eq. (3.6), the average value of the impulse P_1 is zero. Therefore, one only needs to examine P_0 and \mathcal{P}_{vv} terms. Using Eq. (3.7) one can obtain ($k_{\pm} = k \pm q$)

$$\langle P_0 \rangle = \frac{\pi i D}{96} \int dk_+ dk_- \frac{1 - e^{ik_+ k_- z}}{\sinh(\pi k_- / 2)} e^{-ik_- y} \\ \times \frac{1 + k^2 + q^2 + kq}{\cosh(\pi k/2) \cosh(\pi q/2)} \frac{(k-i)(q+i)}{(k+i)^2 (q-i)^2}. \quad (\text{C13})$$

The integral is formed at small values of k_- , and we obtain

$$\langle P_0 \rangle = \frac{\pi D}{24} \int_0^\infty dk_+ \frac{1 + 3k_+^2/4}{(1 + k_+^2/4) \cosh^2(\pi k_+/4)} \approx 0.23D. \quad (\text{C14})$$

The average of the impulse \mathcal{P}_{vv} is ($k_{\pm} = k \pm q$)

$$\langle \mathcal{P}_{vv} \rangle = \frac{\pi D}{96} \int dk dq \frac{q-i}{(q+i)^2} \frac{k+i}{(k-i)^2} e^{ik_- y} \\ \times \frac{1 - e^{-ik_+ k_- z}}{i \sinh(\pi k_- / 2)} \left[-4k_- + \pi(k_-^2 + 4) \coth \frac{\pi k_-}{2} \right] \\ = \frac{\pi D}{12} \int_0^\infty \frac{dp}{(1+p^2) \cosh^2(\pi p/2)} \approx 0.137D. \quad (\text{C15})$$

Thus, the total average impulse is

$$\langle \mathcal{P} \rangle = 2\langle P_0 \rangle + \langle \mathcal{P}_{vv} \rangle \approx 0.6D. \quad (\text{C16})$$

The impulse contribution to the fluctuation of the soliton positions is of the order of D^2 and is negligible in comparison with the contribution Dz , coming from h_3 in Eq. (C12).

-
- [1] R. Ulrich and A. Simon, *Appl. Opt.* **18**, 2241 (1979).
[2] I. P. Kaminow, *IEEE J. Quantum Electron.* **17**, 15 (1981).
[3] C. D. Poole and R. E. Wagner, *Electron. Lett.* **22**, 1029 (1986).
[4] S. C. Rashleigh and R. Ulrich, *Opt. Lett.* **3**, 60 (1978).
[5] S. Machida, I. Sakai, and T. Kimura, *Electron. Lett.* **17**, 494 (1981).
[6] N. S. Bergano, C. D. Poole, and R. E. Wagner, *J. Lightwave Technol.* **5**, 1618 (1987).
[7] D. Andresciani, F. Curti, F. Matera, and B. Daino, *Opt. Lett.* **12**, 844 (1987).
[8] N. Gisin, B. Gisin, J. P. Von der Weid, and R. Passy, *IEEE Photonics Technol. Lett.* **8**, 1671 (1996).
[9] L. E. Nelson, R. M. Jopson, H. Kogelnik, and J. P. Gordon, *Opt. Express* **6**, 158 (2000).
[10] C. D. Poole, *Opt. Lett.* **13**, 687 (1988); **14**, 523 (1989).
[11] C. D. Poole, N. S. Bergano, R. E. Wagner, and H. J. Schulte, *J. Lightwave Technol.* **6**, 1185 (1988).
[12] C. D. Poole, J. H. Winters, and J. A. Nagel, *Opt. Lett.* **16**, 372 (1991).
[13] A. L. Berkhoer and V. E. Zakharov, *Zh. Eksp. Teor. Fiz.* **58**, 903 (1970) [*Sov. Phys. JETP* **31**, 486 (1970)].
[14] C. R. Menyuk, *IEEE J. Quantum Electron.* **25**, 2674 (1989).
[15] P. K. A. Wai, C. R. Menyuk, and H. H. Chen, *Opt. Lett.* **16**, 1231 (1991).
[16] C. R. Menyuk and P. K. A. Wai, *J. Opt. Soc. Am. B* **7**, 1305 (1993).
[17] P. K. A. Wai, W. L. Kath, C. R. Menyuk, and J. W. Zhang, *J. Opt. Soc. Am. B* **14**, 2967 (1997).
[18] S. V. Manakov, *Zh. Eksp. Teor. Fiz.* **65**, 505 (1973) [*Sov. Phys. JETP* **38**, 248 (1974)].
[19] C. R. Menyuk and P. K. A. Wai, *Opt. Lett.* **19**, 1517 (1994).
[20] C. R. Menyuk and P. K. A. Wai, *Opt. Lett.* **20**, 2490 (1995).
[21] C. R. Menyuk and P. K. A. Wai, *J. Lightwave Technol.* **14**, 148 (1996).
[22] I. V. Kolokolov and K. S. Turitsyn, *Zh. Eksp. Teor. Fiz.* **125**, 395 (2004).
[23] T. I. Lakoba and D. J. Kaup, *Phys. Rev. E* **56**, 6147 (1997).
[24] M. Matsumoto, Y. Akagi, and A. Hasegawa, *J. Lightwave Technol.* **15**, 584 (1997).
[25] G. A. Agrawal, *Nonlinear Fiber Optics* (Academic Press, New York, 1995).
[26] M. Chertkov, Y. Chung, A. Dyachenko, I. Gabitov, I. Kolokolov, and V. Lebedev, *Phys. Rev. E* **67**, 036615 (2003).
[27] J. N. Elgin, *Phys. Lett.* **110A**, 441 (1985).
[28] J. P. Gordon and H. A. Haus, *Opt. Lett.* **11**, 665 (1986).
[29] W. Feller, *An Introduction to Probability Theory and Its Applications* (Wiley, New York, 1957).
[30] D. J. Kaup, *Phys. Rev. A* **42**, 5689 (1990).
[31] M. Chertkov, I. Gabitov, I. Kolokolov, and V. Lebedev, *JETP Lett.* **74**, 535 (2001).